Discoloration of Azo-Dyes at Biocompatible pH-Values through an Fe-Histidine Complex Immobilized on Nafion via Fenton-like Processes

S. Parra,[†] V. Nadtotechenko,[†] P. Albers,[‡] and J. Kiwi*[,†]

Laboratory of Photonic and Interfaces, Institute of Molecular Chemistry and Biology, Swiss Federal Institute of Technology, Lausanne 1015, Switzerland, and Degussa AG, Industriepark Wolfgang, Rodensbacher Ch. 4, D-63457, Germany

Received: September 30, 2003; In Final Form: February 2, 2004

The Fe/histidine complex immobilized on a Nafion membrane was employed in the bleaching and photobleaching of the azo-dye Orange II. This photocatalyst shows to be effective in the pH range 3−10. The Fe/histidine/Nafion membrane is able to bleach/photobleach Orange II in the presence of H_2O_2 in a repetitive fashion. The catalyst can be recovered after each cycle and reused for further runs. This Fe/histidine/Nafion membrane was also observed to be surprisingly stable and active toward the oxidation of the azo-dye in the presence of H_2O_2. The percentages of the homogeneous and heterogeneous processes leading to Orange II disappearance on the Fe/histidine/Nafion surface have been quantified as a function of the pH. The results obtained indicate that at pH values > 5.5 heterogeneous catalysis accounts for more than 96% of the Orange II disappearance. The nature of the Fe species (Fe−O−Fe) on the histidine/Nafion surface has been identified and evaluated by Fourier transform infrared spectroscopy (FTIR). The iron content on the Fe/histidine/Nafion membrane was investigated by elemental analysis (EA). No difference was found in the iron content (2.02% w/w) after seven repetitive Orange II discoloration cycles, indicating that leaching of the iron from the Fe/histidine complex does not occur. High-resolution transmission electron microscopy (TEM) revealed iron clusters with a size of ∼6 nm. X-ray photoelectron spectroscopy (XPS) of the Fe complex on the Nafion surface indicated a periodic change in the Fe oxidation state within the photobleaching time of Orange II. The Fe concentration remained fairly stable in the catalyst inner layers as observed by Ar sputtering. This shows that the Fe/histidine complex successfully penetrated some surface layers of the Nafion membrane. Based on the experimental data, a discoloration mechanism of Orange II on Fe/histidine/Nafion membranes is suggested.

Introduction

The present study addresses the preparation, dynamics, and characterization of Fe/histidine immobilized on Nafion. Histidine is an amino acid containing an imidazole ring with the formula $C_3H_4N_2-CH_2-CH(NH_2)-COOH$. The performance of this Fe complex is compared to the performance of the Fe^{3+}/Fe_2O_3/Nafion membranes reported previously for the photocatalytic destruction of Orange II,[1,2] which were effective only up to pH 4.6. This photocatalytic pH limit is given by the range of stability and photoactivity of the hydrocomplex of Fe(III) in an aqueous solution.[3,4] The hydrocomplex (abbreviated as $Fe(OH)^{2+}$)[4−6] refers to the complex ion $[Fe(OH)(H_2O)_5]^{2+}$ that presents two important properties: (a) it shows the highest photodissociation quantum yield under light irradiation in the redox reaction[5,6]

$$Fe(OH)^{2+} + h\nu \rightarrow Fe^{2+} + OH^{\cdot} \qquad (1)$$

and (b) it has been found to be the predominant form for hydrated species of Fe(III) in the 3−4.6 pH range.[3,6]

The advantage of shifting the bleaching/photobleaching activity of the Fe/Nafion photocatalytic membranes[1,2] beyond pH 4.6 to neutral (biocompatible pH values) is to make possible the degradation of organic compounds without the initial adjustment required in the case of Fenton homogeneous pretreatment.[7−9] This is important since a heterogeneous catalyst minimizes the material losses and facilitates the separation of the catalyst from the reaction products at the end of the process,[10,11] compared to the homogeneous catalyzed processes.

We selected the Fe/histidine complex immobilized on Nafion after a long series of preliminary experiments using ligands such as gluconic acid, citric acid, tartaric acid, EDTA, and trietylenetetramine[4] since the Fe/histidine on Nafion proved to have a fast bleaching/photobleaching effect and presented adequate stability during Orange II discoloration. The homogeneous complex of Fe/histidine (1:1) was reported to be active in the oxidation of Indigo-Carmine dye in the presence of H_2O_2.[4,12]

The photocatalytically induced destruction of toxic residues by several macrocyclic complexes immobilized on Nafion membranes has been reported for Co(III) macrocycles,[13] Ru(III) tris-ethylenediamine,[14] Pd-phenanthroline complexes immobilized,[15] and tetraphenyl-porphyrin derivatives films.[16] Nafion is an optically transparent polymer consisting of a perfluorinated backbone connected to sulfonic groups through short chains of perfluoro-propylene ether. This polymer has an inverted micelle structure with polar cavities of about 40 Å where the pendant SO_3^- groups are located.

This study describes in a detailed form the discoloration of the azo-dye Orange II by a novel Fe/histidine/Nafion heterogeneous catalyst and examines the kinetics, stability, and the

* Corresponding author.
[†] Swiss Federal Institute of Technology.
[‡] Degussa AG.

10.1021/jp031127o CCC: $27.50
Published on Web 03/13/2004

effects of the solution parameters on the discoloration of Orange II. A detailed study of the Fe nanoclusters on the Nafion surface was carried out by FTIR, TEM, XPS, and EA. A suitable method is presented to assess the percentage of the homogeneous and of the heterogeneous processes leading to Orange II disappearance on the Fe/histidine/Nafion surface at different pH values.

Experimental Section

Preparation of the Nafion Membrane Incorporating Fe/Histidine. The Nafion perfluorinated membrane (Dupont N°117, 0.007 in. thick, Aldrich No 7,467-4) was first washed with a mixture of H_2O_2/H_2SO_4 and then rinsed with deionized water to clean the surface from residual organic contaminants. The clean Nafion membrane was then exchanged for 2 h with Fe^{3+} and histidine in a solution containing 10 mM Fe^{3+} ions and 12 mM histidine. During this period the spectrum of the Fe/histidine solution was monitored and seen to decrease due to the partial adsorption of Fe/histidine onto the Nafion. The immobilization during the in situ formation of the complex on the Nafion increased the stability of the Fe/histidine species with respect to the homogeneous Fe/histidine with the same composition. The spectrum of the Fe/histidine/Nafion membrane shows a characteristic maximum at 440 nm. Different molar ratios of the two reactants in solution were tried. In the presence of Nafion, a ratio of histidine/Fe of 1:5 attained the best discoloration kinetics of Orange II in the dark and under light irradiation. After the exchange, the Fe/histidine/Nafion-loaded membrane was washed thoroughly with deionized water. The Fe content of the Fe/histidine/Nafion membrane was determined by elemental analysis (EA). The Fe content before and after the photocatalytical discoloration of Orange II was found to be 2.02% in w/w loading of Fe onto the Nafion.

The analytical grade reagents H_2O_2, Orange II, HNO_3, $Fe(NO_3)_3 \cdot 9\ H_2O$ were from Fluka (Buchs, Switzerland) and FerroZine Aldrich 16,060-1 and were used as received.

Experimental Procedures and Operating Conditions. The catalytic activity of the Fe/histidine/Nafion was investigated using Orange II solutions as a model azo-dye under irradiation from a lamp emitting light in the visible region. The photochemical reactor consisted of 80 mL cylindrical Pyrex flasks each containing 60 mL of solution. A 48 cm^2 strip of the Fe/histidine/Nafion membrane was placed immediately behind the wall of the reaction vessel to carry out the photochemical experiments. The irradiation of samples was carried out in the cavity of a Hanau Suntest solar simulator air-cooled at 45° C. The Suntest lamp had a wavelength distribution with 7% of the photons between 290 and 400 nm. The profile of the photons emitted between $\lambda = 400-800$ nm followed the solar spectrum. The Suntest solar simulator was tuned to light intensities of 50, 70, and 90 mW/cm^2. 50 mW/cm^2 corresponds to 50% of the light intensity of the midday equatorial solar radiation (AM 1). The radiant flux was monitored by a power-meter of LSI Corporation, Yellow Springs, CO. This gave the envelope for the total radiant flux allowed at different settings and permitted us to vary the number of photons reaching the Fe/histidine/Nafion membrane and to monitor the photocatalytic process under different light intensities.

Analyses of Irradiated Solutions. Spectrophotometric analyses of the model organic compound Orange II solutions were carried out by a Hewlett-Packard 8452 diode-array spectrophotometer at the maximum of the Orange II absorbance ($\lambda = 486$ nm). The same instrument was used for the detection of the total iron concentration (Fe^{2+} and Fe^{3+}) in an irradiated solution by complexation with Ferro-Zine in the presence of hydroxylamine.[17] The total organic carbon (TOC) determination was carried out by a Shimadzu 500 instrument equipped with an ASI automatic sample injection. The peroxide concentration in solutions was assessed by Merkoquant paper and found to be at levels between 0.5 and 25 mg/L in aqueous solutions.

Fourier Transform Infrared Spectroscopy (FTIR). The detailed description of the applied external reflection FTIR technique and procedure used has been previously reported.[18] The infrared reflection spectra of catalyst samples were recorded on a Bruker IFS55 FTIR spectrometer equipped with a MCT detector and a reflection attachment (Seagull). A wire-grid polarizer was placed before the sample and provided p- or s-polarized light. These accessories were from Harrick Scientific Co. It was found for the system under investigation that the most informative reflection spectra could be recorded by the use of p-polarized light and an angle of incidence of 20°. The unit of intensity is defined as $-\log(R/R_o)$, where R_o and R are the reflectivities of the catalyst sample after reaction and before reaction directly after its preparation, respectively. Both sample and reference spectra were averaged over the same number of 1000 scans.

X-ray Photoelectron Spectroscopy (XPS). Measurements were carried out in a Leybold-Heraeus instrument calibrating the binding energies (BE) to the $Auf_{7/2}$ level taken as 84.0 eV. The electron energy analyzer (Leybold EA 11A) was operated at a band-pass energy of 75 eV in the fixed analyzer transmission mode. The evaluation of the binding energies of the embedded Fe clusters was carried out following the DIN norms[19] and after taking into consideration the sensitivity factors allowed a reproducibility of ±5% in the measurements. An ADS 100 set was used to evaluate the XPS data by subtracting the X-ray satellites and correcting the data by the relative sensitive factors, according to Shirley.[20] The presence of electrostatic charging effects was controlled by additional measurements including charge compensation by changing the electrostatic potential at the entrance aperture of the electron energy analyzer.

Transmission Electron Microscopy (TEM). A field emission TEM, the Philips CM 120 microscope was used to observe the Fe clusters on the Nafion surface. The Nafion was coated with epoxy resin and the fabric was cut with a microtome to a thin layer of 50 nm at a 90° angle for the experimental observations. The instrument used for electron microscopy (120 kV, 0.35 nm point resolution) was equipped with an energy-dispersive X-ray analysis EDX to identify the Fe clusters and other species on the Nafion membrane.

Results and Discussions

Performance of the Fe/Histidine/Nafion Membrane During Orange Discoloration vs Fenton Homogeneous Processes. Figure 1a shows the partial discoloration of an Orange II solution (0.15 mM) under visible light irradiation in a homogeneous solution in the presence of the Fenton reagent (Fe^{3+}/H_2O_2). This discoloration was photocatalyzed by Fe^{3+} ions with a concentration of 0.5 mg/L of iron ions. This concentration was higher than the 0.42 mg/L leaching out when using an Fe/histidine/Nafion membrane to catalyze the discoloration under light as shown in Figure 1c. The photocatalysis mediated by Nafion/Fe ion at pH 4.6 is presented in Figure 1b. The results presented in Figure 1c show that within 30 min the discoloration of Orange II proceeds due to the Fe/histidine/Nafion membrane and only to a very small extent to the Fenton homogeneous side reaction shown in Figure 1a.

Figure 2 shows the results obtained from control experiments in the dark during Orange discoloration in the presence of H_2O_2.

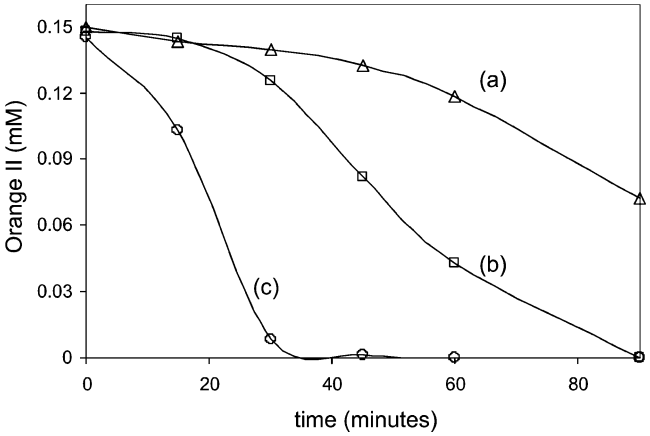

Figure 1. Discoloration of an Orange II (0.15 mM) solution at initial pH 4.6 (natural pH) in the presence of H_2O_2 (10 mM) and (a) 0.5 mg/L Fe ions in homogeneous Fenton processes using light irradiation from a Suntest sunlight simulator with an intensity of 90 mW/cm^2, (b) Nafion/Fe ion membrane under light irradiation, and (c) Fe/histidine/Nafion membrane under light irradiation.

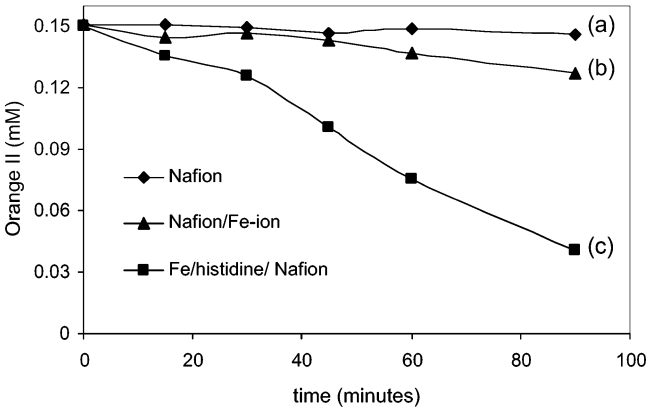

Figure 2. Discoloration in the dark of an Orange II (0.15 mM) solution at an initial pH 4.6 (natural pH) in the presence of H_2O_2 (10 mM) and (a) Nafion membrane, (b) Nafion/Fe ion membrane, and (c) Fe/histidine/Nafion membrane.

The results in Figure 2a indicate that the Nafion membrane alone does not catalyze the discoloration of the dye. Figure 2b shows that the Nafion/Fe-ion[1] membrane leads only to a very modest discoloration of the dye. It is seen in Figure 2c that Orange II discoloration attains ~60% after 90 min reaction. The discoloration kinetics and efficiency are seen to be much lower than that reported in Figure 1c for the same system under visible light irradiation.

Kinetics of Orange II Discoloration as a Function of the Initial pH. Figure 3 shows the dye disappearance under irradiation from a Suntest lamp mediated by an Fe/histidine/Nafion membrane as a function of the initial pH of the solution. The amounts of Fe^{3+} ion found after each experiment are: pH 3.1 (0.31 mg/L), pH 4.6 (0.42 mg/L), pH 7.2 (0.36 mg/L), pH 9.0 (0.47 mg/L), and finally pH 10.2 (0.36 mg/L). These values suggest that no Fe-ions leach into the solution from the Fe/histidine/Nafion surface and that the Fe originates from the Nafion surface, from impurities of Orange II, or from the reagents used. The kinetics for the discoloration processes are seen to decrease as the initial pH increases from 3.1 up to 10.2. The complex shape for the Orange II concentration as a function of time suggests the presence of pH dependent transient intermediates affecting the course of Orange II disappearance. Iron did not precipitate from the Fe/histidine/Nafion complex at pH > 4.6, as was the case for the Nafion/Fe exchanged

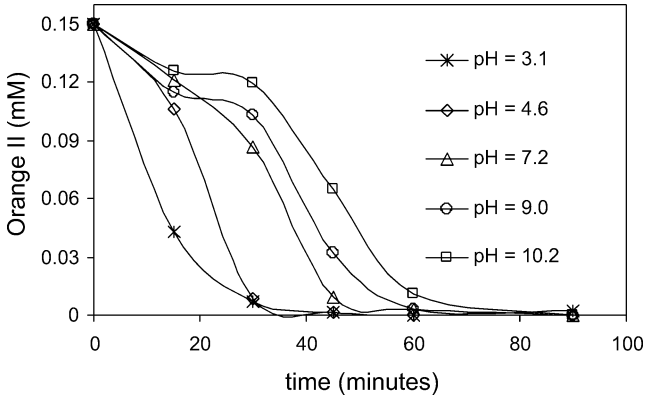

Figure 3. Discoloration of an Orange II (0.15 mM) solution under a Suntest lamp in the presence of H_2O_2 (10 mM) mediated by an Fe/histidine/Nafion membrane as a function of the initial pH of the solution.

TABLE 1: Pseudo-First-Order Rate Constants and Percentage of Homogeneous and Heterogeneous Catalysis for the Discoloration of Orange II (0.15 mM) as a Function of pH

pH	K_{obs} (s^{-1})	K_{homo} (s^{-1})	K_{hetero} (s^{-1})	P_{homo} (%)	P_{hetero} (%)
2.5	1.62×10^{-3}	4.72×10^{-4}	1.15×10^{-3}	29	71
3.3	1.39×10^{-3}	2.65×10^{-4}	1.13×10^{-3}	19	81
4.1	8.07×10^{-4}	1.97×10^{-4}	6.10×10^{-4}	24	76
4.6	3.80×10^{-4}	9.18×10^{-5}	2.88×10^{-4}	24	76
5.5	2.93×10^{-4}	1.17×10^{-5}	2.82×10^{-4}	4	96

membranes reported previously.[1] This observation is interesting since it is well-known that the stability of Fe-coordination complexes in alkaline media is poor in the presence of peroxides.[21a] In Figure 3, the catalysis leading to Orange II disappearance is seen to be effective up to pH 10.2, which suggests that we do not have a classical Fe/histidine complex on the Nafion surface, but a different form of stable Fe ion cluster(s) compared to the one previously reported.[1] The local pH at microheterogeneous surfaces has been reported to be 3-4 units below the bulk solution.[21b] This effect may also play an important part in the electrostatic traction between the Nafion surface and the Fe/histidine complex.

Extent of the Homogeneous and Heterogeneous Catalyses. To assess the extent of the homogeneous catalysis leading to Orange II oxidation, several experiments were performed in homogeneous solution with 0.5 mg/L of Fe^{3+} ions at different pH values. This iron concentration was higher than the concentration of iron ions leaching out in solution after Orange II discoloration as described in the paragraph above and was to estimate the participation of the homogeneous catalysis in the overall process within the pH range of 2.5−5.5. Table 1 shows the pseudo-first-order rate constants calculated by fitting the degradation results under these experimental conditions. To distinguish the contribution of heterogeneous and homogeneous catalyses during Orange II discoloration, the initial slopes of the traces in Figure 3 were quantified. This made possible to consider the competing reactions

$$\text{Orange II} + H_2O_2 + \text{Fe/histidine/Nafion} \rightarrow \text{oxidation products} \quad k_{hetero} \quad (2)$$

$$\text{Orange II} + H_2O_2 + Fe^{2+} \rightarrow \text{oxidation products} \quad k_{homo} \quad (3)$$

where k_{hetero} and k_{homo} are the pseudo-first-order rate constants for heterogeneous and homogeneous catalyses, respectively. Therefore, the observed rate constant becomes

$$k_{obs} = k_{hetero} + k_{homo} \quad (4)$$

The contribution of heterogeneous catalyses (k_{hetero}) can be estimated once the rate constant of the homogeneous reactions are known from eq 5

$$P_{hetero} = \frac{k_{hetero}}{k_{obs}} \times 100 = \frac{k_{obs} - k_{homo}}{k_{obs}} \times 100 \quad (5)$$

where P_{hetero} is the percentage of the heterogeneous catalysis during the degradation of the Orange II. The k_{homo} values obtained by homogeneous phase experiments with 0.5 mg/L of iron were used to identify the contribution of the homogeneous oxidation since this is the highest concentration of Fe^{3+} ions generated at different pH values after 90 min. This iron concentration was chosen as the reference value for homogeneous degradation shown in Figure 1a. Table 1 shows the pseudo-first-order rate constants and the percentages of heterogeneous and homogeneous catalyses and the heterogeneous process represents 76% of the overall degradation at pH 4.6 and 96% at pH 5.5. These results suggest that in the biocompatible pH range (pH 6−8) the Orange II discoloration proceeds practically by heterogeneous Fe/histidine/Nafion-mediated processes.

At a low pH, the $OH^{\bullet}$ radicals are generated by the reaction[3,7,8]

$$Fe^{2+}(aq) + H_2O_2 \rightarrow Fe^{3+}(aq) + OH^{\bullet} + OH^{-} \quad (6)$$

whereas at a neutral or an alkaline pH (Figure 3) the iron is bound, showing less reactivity as a ferryl complex L_nFe^{IV} via reaction 7[4,8,11]

$$L_nFe^{IV} + H_2O_2 \rightarrow (L_nFe^{IV}{=}O) + H_2O \quad (7)$$

pH Drift during Orange II Discoloration. Figure 4 shows that the decrease of pH for Orange II solutions is very significant within the first 15 min of the reaction. This implies that the intermediates required for the dye photobleaching are only effective at acidic pH values $\leq$ 4.[9,10,22] The discoloration mechanism involves the formation of short-chain carboxylic acids[9,22] in the step preceding CO_2 evolution. The pK_a value of the C_1-C_6 acids (branched or not) is predominantly in the pH range 3−4, which corresponds to pH values after 20 min as shown in Figure 4.

At more basic pH values, the species $Fe(H_2O)_6^{3+}$ and $Fe(H_2O)_5OH^{2+}$ (in shorthand notation $Fe(OH)^{2+}$) dehydrate rapidly to $Fe(H_2O)_4OH^{2+}$. This species[23] deprives the Fe^{3+} ion of its complete six-coordinated hydration shell that is needed during the discoloration of Orange II as shown in Figure 3. In homogeneous solution the Fenton process proceeds optimally at pH 3 due to the presence of the complete hydration shell of the iron at this pH since the catalysis goes through hydrated Fe ions.[4,9,23] In addition, at acidic pH-values, the $OH^{\bullet}$ radical is the dominant species of the H_2O_2 decomposition catalyzed by Fe ions.[3,6,8] Recently, the adduct formation between $OH^{\bullet}$ and Orange II during Orange II decomposition at acidic pH values involving protonated species has been reported.[9,10]

Long Term Performance of the Fe/histidine/Nafion Membranes during Orange II Discoloration. Figure 5 shows the catalytic nature of the Orange II discoloration, which can recycle up to seven times on the Fe/histidine/Nafion membrane. No variation in the catalyst performance was observed in regard to the kinetics or efficiency of the process. After each recycling the catalyst was thoroughly washed with distilled water. Then, Orange II and H_2O_2 were added before the next discoloration run.

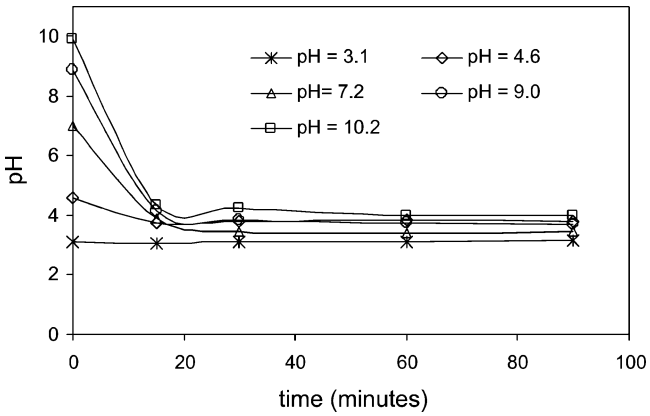

Figure 4. Evolution of pH during the discoloration of an Orange II (0.15 mM) solution under a Suntest lamp in the presence of H_2O_2 (10 mM) mediated by an Fe/histidine/Nafion membrane.

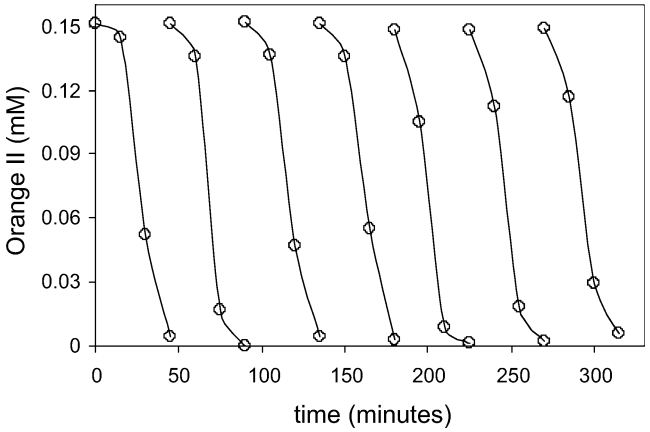

Figure 5. Repetitive photocatalytic discoloration of an Orange II (0.15 mM) solution at initial pH 4.6 (natural pH) under Suntest light irradiation (90 mW/cm^2) in the presence of H_2O_2 (10 mM) and an Fe/histidine/Nafion membrane.

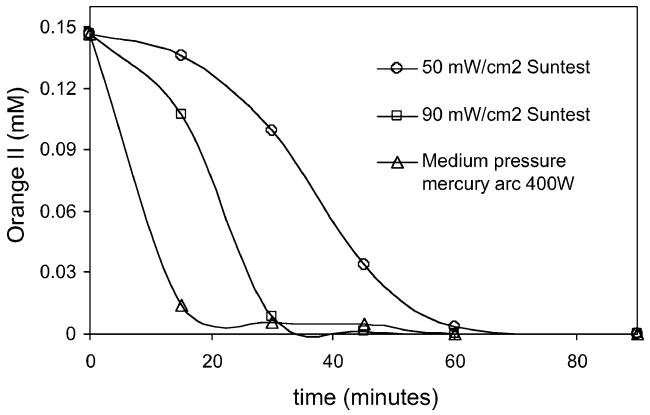

Figure 6. Reduction of the Orange II concentration in a solution containing H_2O_2 (10 mM) in the presence of an Fe/histidine/Nafion membrane as a function of the type of light and the intensity of the light used.

Kinetics of the Dye Discoloration as a Function of Light Intensity, H_2O_2 Concentration, and Orange II. Figure 6 shows the discoloration of Orange II as a function of light intensity. The discoloration is more efficient as the intensity of the applied light is increased. Orange II samples under Suntest light irradiation did not reach the saturation limit as a photo-

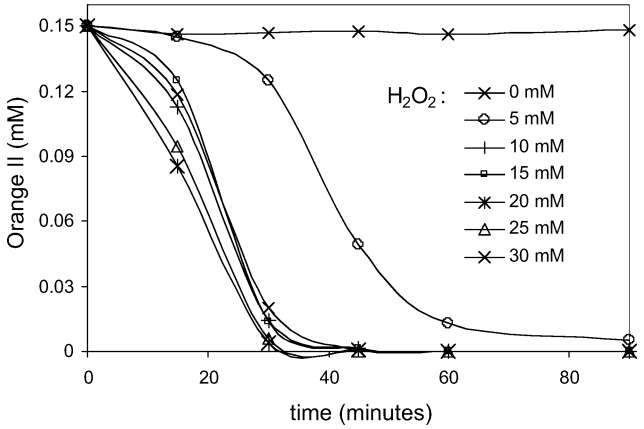

Figure 7. Discoloration of Orange II (0.15 mM) as a function of H_2O_2 concentration at an initial pH 4.6 in the presence of an Fe/histidine/Nafion membrane under Suntest light irradiation.

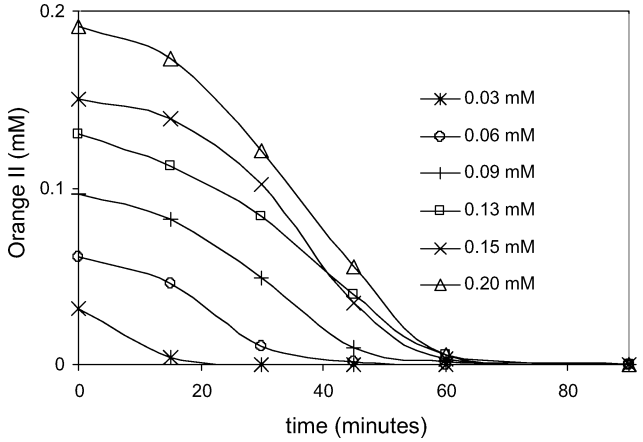

Figure 8. Kinetics of Orange II discoloration at different concentrations at an initial pH 5.1 in the presence of H_2O_2 (10 mM) under Suntest light irradiation (50 mW/cm^2) mediated by an Fe/histidine/Nafion membrane.

sensitizer for reactions catalyzed by the Fe/histidine/Nafion membrane since the discoloration is a function of the intensity of the applied light. It was not possible to predict if there were enough Fe-chromophore active sites on the Nafion to absorb the Suntest light (2×10^{16} photons/s) since the 6 nm Fe clusters shown below by transmission electron microscopy (TEM) present a nonuniform distribution on the Fe/histidine/Nafion membrane. The discoloration of Orange II under a medium-pressure mercury arc with a light intensity of 5×10^{19} photons/s (366 nm) was seen to proceed at a much faster rate than under Suntest visible light irradiation, reaching completion in under 20 min.

The effect of H_2O_2 concentration on Orange II degradation was seen to be important experimentally and is presented in Figure 7. When H_2O_2 was absent no Orange II discoloration was observed in the dark. When a 5 mM H_2O_2 concentration was added, Orange II discoloration was possible and the rate of discoloration attained a limit for H_2O_2 concentrations of 10 mM and above. Beyond 10 mM, the discoloration rate does not become faster since the propagation step in the oxidative chain would be hindered by excess H_2O_2 scavenging the $OH^\bullet$ radicals in solution[7,8]

$$H_2O_2 + OH^\bullet \rightarrow H_2O + HO_2^\bullet \quad (8)$$

The discoloration of Orange II was investigated at different initial dye concentrations, and the results are presented in Figure 8. A steeper decline for higher concentrations of Orange II, due to the positive effect of the dye concentration on the reaction rate, is observed in Figure 8, providing the evidence for a mass transfer controlled process. The mass transfer is driven by the difference in the Orange II concentration existing between the bulk solution and the Nafion membrane. The diffusion length (x) of the oxidative radical from the Fe/histidine/Nafion membrane can be estimated from the Smoluchowski diffusion relation

$$x^2 \sim D\tau \quad (9)$$

The reaction rate between the $OH^\bullet$ radicals in solution and Orange II has been recently reported to be close to 10^9 M^{-1} s^{-1}.[9,10] At a 0.20 mM concentration of Orange II, the lifetime of the encounter pair is $\sim 10^{-6}$ s. With $D \sim 5 \times 10^{-6}$ cm^2/s, a value for the diffusion length (x) of $\sim$50 nm in eq 7 is found for the $OH^\bullet$ radical. In the case of the $HO_2^\bullet$ radicals, the value of the reaction rate of $HO_2^\bullet$ with Orange II is $\sim 10^6$ M^{-1} s^{-1}. From this a value of $\sim$310 nm can be estimated for the diffusion length of the $HO_2^\bullet$ radical from the Fe/histidine/Nafion membrane.

Infrared Spectroscopy during Orange II Discoloration. The FTIR of a Nafion-H^+ membrane with Fe(III) complex is shown in Figure 9a. The spectrum found is similar to the one reported for Nafion cationic membrane.[24] Figure 9a (trace 1) shows the spectrum of the Nafion-H^+ membrane loaded with Fe_2O_3[2]. The spectra in traces 2 and 3 show Fe/histidine/Nafion membranes before and after discoloring Orange II. In the spectra reported in Figure 9a, it is possible to see (a) strong C−F symmetric and anti-symmetric vibrations in the 1400−1100 cm^{-1} region, (b) C−F stretching vibration at 623 cm^{-1}, and (c) SO_3^- symmetric stretching band at 1056 cm^{-1}.

Figure 9b (trace 1) shows the differential spectrum of the Fe(III) complexes consisting mainly of Nafion/histidine and a certain amount of Fe_2O_3 with respect to the Nafion-H^+ membrane. The incorporation of Fe into the Nafion leads to disturbances of the vibrational bands of C−F (1213 and 1147 cm^{-1}) and $-SO_3^-$ (1062 cm^{-1}), probably due to the binding of Fe(III) to the SO_3^- pendant groups of the Gierke cages. The band at 629.6 cm^{-1} is due to the disturbance of the C−F vibrational bands with the formation of some hematite (625 cm^{-1}) and additional modifications of the Nafion C−F bands due to the Fe-histidine binding of the $-SO_3^-$ groups. The weak band at 870 cm^{-1} corresponds to the Fe−O−Fe vibration.[10] After the Fe/histidine was exchanged on Nafion, new bands appeared at 2920 and 2850 cm^{-1} due to CH_3 and CH_2 vibrations.

Figure 9b (trace 2) shows the differential spectrum of an Fe/histidine/Nafion membrane respect to the Fe ion/Fe_2O_3/Nafion. The band at 873 cm^{-1} indicates that the addition of histidine decreases the concentration of the Fe−O−Fe species relative to the concentration found in the Fe ion/Fe_2O_3/Nafion membrane.

Figure 9b (trace 3) shows the differential spectrum of the Fe/histidine/Nafion membrane after the discoloration of Orange II with respect to the same membrane before use. The changes in the membrane can be found in (a) bands at 1054.0 cm^{-1} ascribed to $-SO_3^-$ and (b) C−F polymer bands at 1192 and 1130 cm^{-1}. New bands appear at 2920 and 2850 cm^{-1} due to CH_3 and CH_2 vibrations indicating organic intermediate formation on the membrane surface.

X-ray Photoelectron Spectroscopy (XPS) of the Fe/Histidine/Nafion Membrane Active in Orange II Discoloration. Table 2 shows that the Fe content in the topmost layer

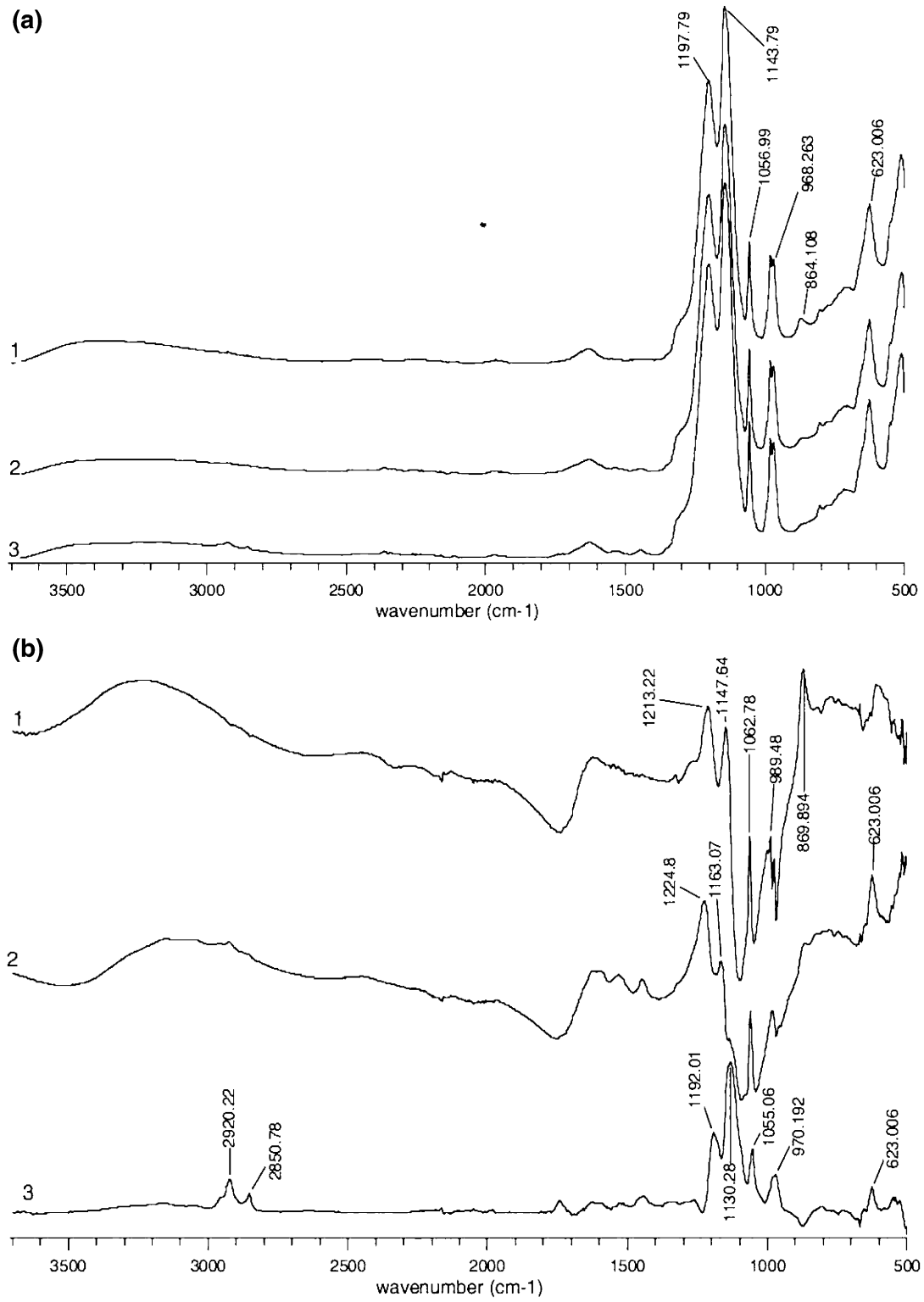

Figure 9. (a) (trace 1) FTIR spectum of Nafion-H^+ membranes with Fe_2O_3; (trace 2) Nafion-H^+ loaded with Fe/histidine before discoloration of Orange II; (trace 3) Nafion-H^+ loaded with Fe/histidine after discoloration of Orange II. (b) (trace 1) Differential spectrum of Nafion loaded with Fe_2O_3 with respect to a Nafion-H^+ membrane; (trace 2) differential spectrum of Fe/histidine/Nafion membrane with respect to an Fe^- ion/Fe_2O_3/Nafion membrane; (trace 3) differential spectrum of Fe/histidine/Nafion membrane after Orange II discoloration with respect to the same membrane before use.

decreases during the photocatalysis leading to Orange II photobleaching under the experimental conditions used in Figure 1c but keeps quite constant after 30 min (see Table 2). This suggests that after some initial Fe loss a good adhesion between the iron and the Nafion has been attained in the Fe/histidine/Nafion membrane. In Table 2, the N is present as an ammonium species. The S is present as sulfonate with a binding energy of BE 160 eV in the oxidative media of the reaction. Also, organic sulfur species with peaks at BE 164/165 eV were observed. The binding energy values (signal maxima) in Table 3 suggests that the initial Fe(III) undergoes redox reactions within the degradation time of Orange II of the type Fe(III)→ Fe(II) → Fe(III).[27,28] These redox reactions have been described as $[RCO_2{-}Fe]^{2+} \rightarrow [R^{\bullet}] + CO_2 + Fe^{2+}$.

TABLE 2: Percentage Composition of the Topmost Layer of the Fe/Histidine/Nafion Membrane Found by XPS at Different Times during Orange II Discoloration under Light in Presence of H_2O_2

	Nafion Fe zero time	Nafion Fe 30 min	Nafion Fe end of reaction 1h
	123	124	125
C 1s	46.70	59.40	61.70
N 1s	2.13	4.37	3.77
O 1s	11.50	20.50	22.00
F 1s	37.70	12.80	9.24
Al 2p			0.20
Si 2p	0.73	1.81	1.96
S 2p	0.54	0.73	0.66
Ca 2p	0.04		
Fe 2p	0.72	0.35	0.37
Zn $2p_{3/2}$			0.08

TABLE 3: Binding Energy Values of the Signal Maxima in EV

	Nafion Fe zero time	Nafion Fe 30 min	Nafion Fe end of reaction 1h
	123	124	125
C 1s	290.5/285.0	285.0	285.0
N 1s	399.9	400.3	400.2
O 1s	534.6/531.9	534.2/531.7	534.2/531.8
F 1s	688.7	688.9	689.2
Al 2p			74.8
Si 2p	103.2	101.6	101.6
S 2p	169.3/164.3	169.2/164.9	169.1/164.5
Ca 2p	348.9		
Fe 2p	712.6	712.0	712.4
Zn $2p_{3/2}$			1020.5

SCHEME 1

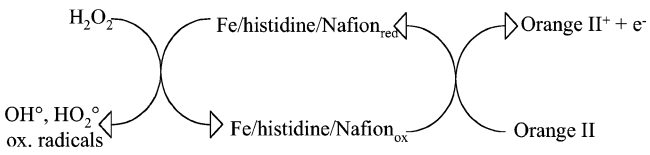

Figures 10a,b,c present the XPS profile data of the stripping due to Ar ion sputtering of the Fe/histidine/Nafion membrane consisting of 40 spectra arranged in 3D plots of ~2 Å each in order of increasing depth. In each case the XPS− spectrogram has been focused on the binding energy (BE) of a different element of the membrane. In Figure 10a, it is seen that the Fe concentration increases with depth in the topmost layers of the Nafion membrane remaining stable afterward. This means that the Fe/histidine complex impregnation has successfully penetrated into the Nafion membrane. Figure 10b shows that the oxygen concentration profile decreases from the topmost layers down to the inner catalyst layers. This means that the surface layers involving oxygenated species carry the oxidation of Orange II and that these O-containing species remain absent in the inner layers of the Fe/histidine/Nafion membrane. Figure 10c shows the S-concentration profile decreasing with depth. This means that the S-content of the Orange II is destroyed during the photocatalysis in the few topmost layers on the Fe/histidine/Nafion membrane. The sulfonate species coexist in the surface region with organic sulfur as seen from the BE energies. Changes in the fine structure of the C signal were also observed as a function of depth. In the topmost layer, a significant peak of CF_3^- at about 292 eV was observed. After sputtering, CF_2^- and CF^- species appear close to 292 eV. This means that a different chemistry was taking place during Orange II discoloration in the topmost layer and in the inner catalyst layers. Aliphatic CH− species were observed at 285 eV along with CO− species at 286/287 eV.

High-Resolution Transmission Electron Microscopy (HR-TEM) of the Fe/Histidine/Nafion Membranes. Figure 11a shows the continuous iron layer on the Nafion membrane. The iron cluster layer is seen to penetrate the Nafion membrane within the length of the Nafion membrane. Figure 11b shows the fairly homogeneous distribution of iron clusters on the Nafion surface with size 5−7 nm (centered at ~6 nm). These iron clusters seem to consist of Fe agglomerates and are not due to metallic Fe as shown by the low contrast between the iron clusters and the Nafion in Figure 11b. The cluster size and shape did not vary during long-term repetitive use of the Fe/histidine/Nafion discoloration of Orange II. From the size of the Fe-clusters shown in Figure 11b (~6 nm), the formation of iron monomers or dimers is seen to be preferred compared to larger iron agglomerates.

Figure 11c shows the energy-dispersive X-ray analysis (EDX) identifying the Fe on the Cu-grid. The Fe, F, C, and O on the left-hand side of the spectrogram correspond to the main elements at the Fe/histidine/Nafion surface. The Cu stray signal from the supporting grid is seen at the right-hand side of the Fe peaks. The minor components detected on the surface are K, Cl, Si, and Cu. The Fe peak is seen to overlap with the F peak. Evidence for FeF_2 (ICSD 202047) was found in the samples as reported previously.[10] The formation of FeF_2 cannot be attributed to the reaction between Fe^{3+} and fluorine from the Nafion during the ion exchange due to thermodynamic reasons since we have to take into consideration the strong C−F bond existing in the Nafion. The FeF_2 is suggested to form in reaction 11 due to the action of the electronic beam applied during electron microscopy. All efforts were made to minimize this effect during the time of observation by defocusing the electronic beam. The atomic % of C, F, and Fe on the Fe/histidine/Nafion at time zero are 69.9, 26.0, and 4.1, respectively. Due to reactions 10 and 11 below, the F component surface decreases during the observation time, and after one minute the atomic % of C, F, and Fe becomes 55.3, 11.9, and 32.8.

$$e^- + >C{-}F \rightarrow F^- + >C^\bullet \quad (10)$$

$$Fe^{3+} + F^- \rightarrow FeF^{2+} \quad (11)$$

Mechanism of Discoloration of Orange II in the Presence of the Fe/Histidine/Nafion Membrane. The most suitable discoloration of Orange II was obtained with an Fe/histidine 5:1 species, possibly consisting of multi-metal clusters of different iron species. The spectrum of the Fe/histidine/Nafion presented some of the features of the Fe/histidine complex, in particular the formation of the characteristic Fe/histidine peak at $\lambda = 460$ nm.[25] To explain the unusual composition of the Fe/histidine on the Nafion matrix producing the optimal Orange II discoloration, we suggest that the addition of the histidine to the Fe^{3+} solution leads to the formation of highly charged in situ Fe/histidine clusters on the Nafion surface. This allows (a) the formation of the suitable precursor for the deposition of iron clusters having different properties compared to Fe^{3+} ions exchanged on Nafion[1] and (b) the increased accessibility of the Nafion sulfonic groups toward Fe^{3+} ions, improving the exchange capacity of the Nafion due to a stronger matrix effect on the Q-sized Fe clusters.[26]

The photocatalytic reaction mechanism of Orange II discoloration on Fe/histidine/Nafion membranes in the presence of peroxide is suggested in Scheme 1. During each cycle, the Fe/

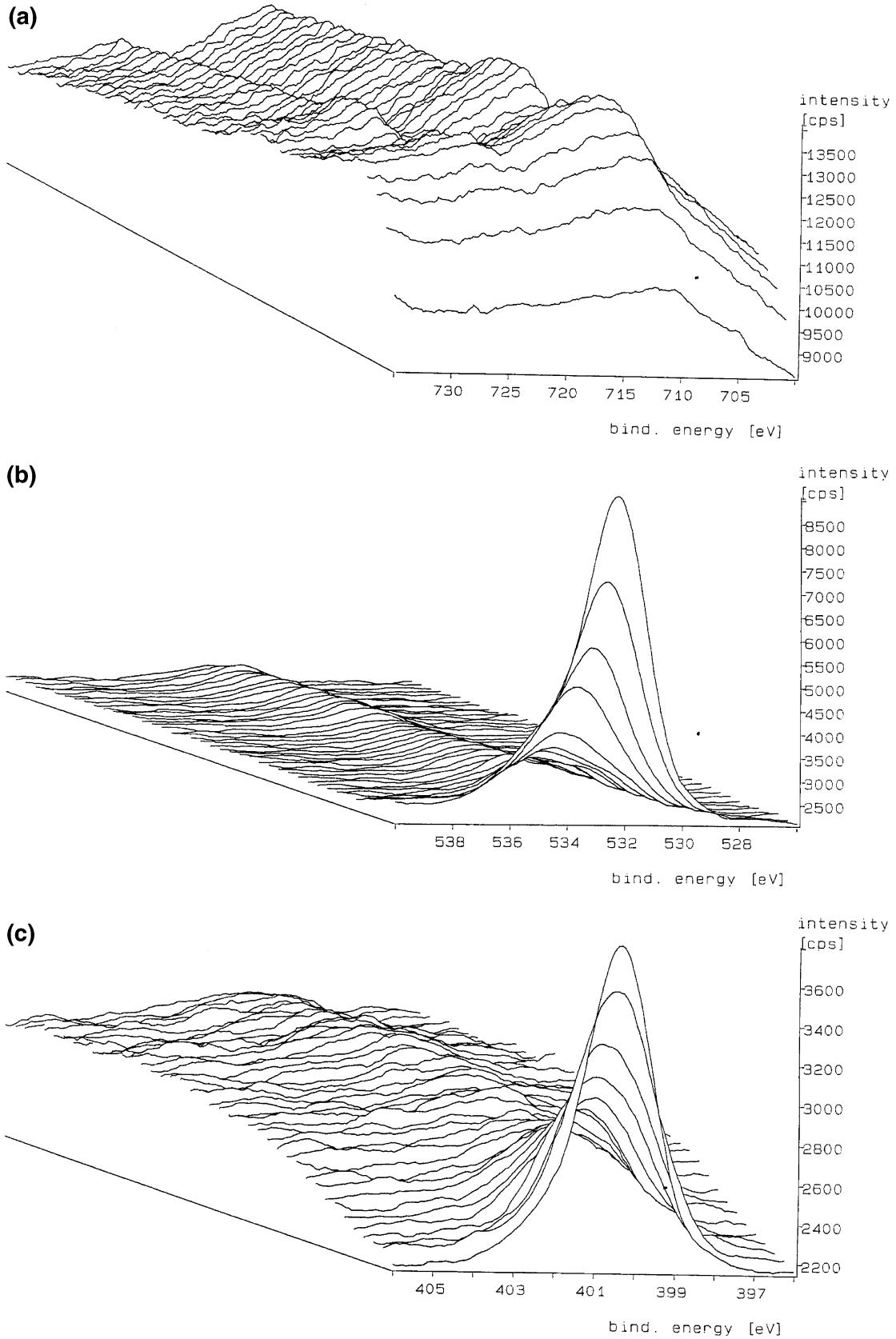

Figure 10. (a) Fe species as a function of the stripping depth during Ar ion sputtering of the Fe/histidine/Nafion membrane surface. (b) O-containing species as a function of the stripping depth during Ar ion sputtering of the Fe/histidine/Nafion membrane surface. (c) S species as a function of the stripping depth during Ar ion sputtering of the Fe/histidine/Nafion membrane surface.

histidine/Nafion$_{ox}$ would be reduced to the more active Fe/histidine/Nafion$_{red}$ containing some Fe(II) as found by XPS measurements, while Orange II in the right-hand side of Scheme 1 is oxidized with the concommitant reduction of H_2O_2. The stable final products of Orange II decomposition have been reported[31] as CO_2, acetic acid, formic acid, glioxalic acid, and small quantities of 1,3-isobenzofurandione and 4-hydroxybenzenesulfonic acid.

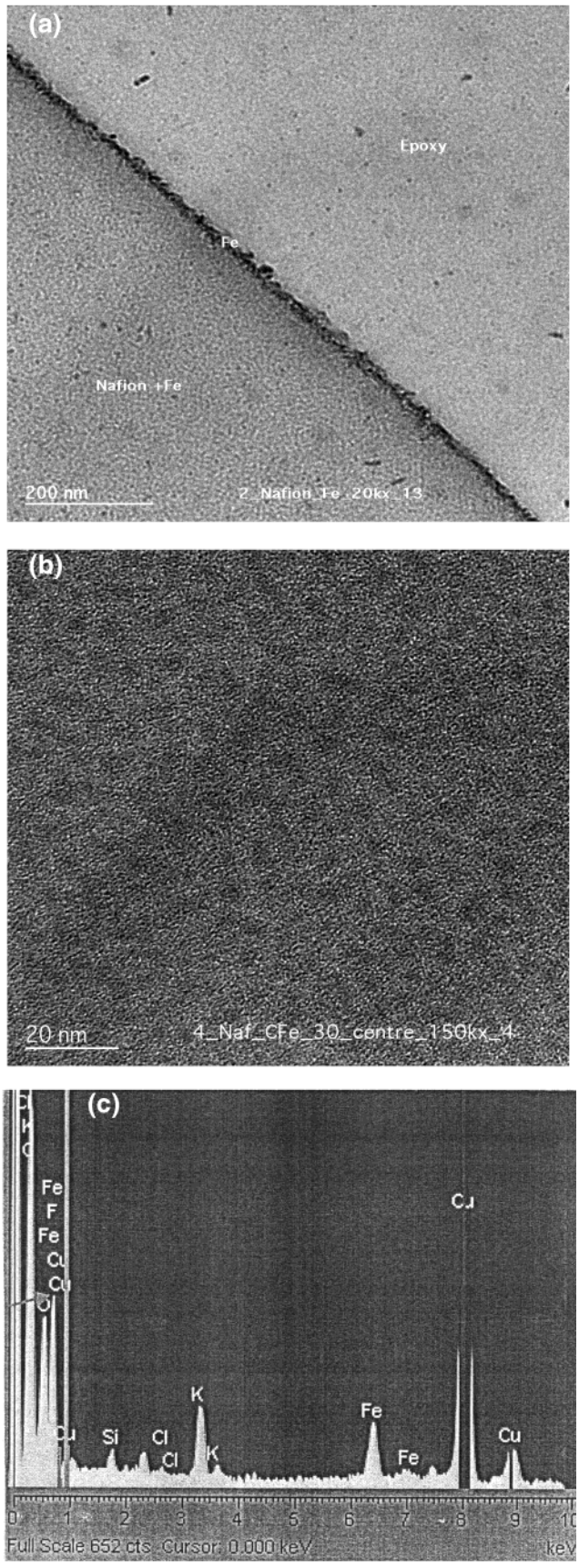

Figure 11. (a) Transmission electron microscopy (TEM) of the Fe/histidine/Nafion membrane showing the continuous layer of Fe clusters. (b) Fe cluster distribution on the Nafion membrane. (c) Energy-dispersive X-ray spectrogram (EDX) of the Fe/histidine/Nafion on a Cu grid showing the elements on the Nafion membrane surface.

The histidine ligands do not undergo chemical changes within the photoredox reactions of Fe(III), as can be seen from the results reported in Figure 5. The histidine molecule presents three coordination sites: (a) the carboxylic group ($pK_a = 1.9$), (b) the imidazole nitrogen ($pK_a = 6.1$), and (c) the amino nitrogen ($pK_a = 9.1$). A more favorable pH for complexation in aqueous solution becomes available as the pH increases. The potential 0.77 eV of Fe(III)/Fe(II) is reduced by ligands such as imidazole since these negative ligands are π-electron acceptors or stronger σ donors than water or amines.[21a,29] By X-ray diffraction studies, histidine has been reported to coordinate with Fe, Mn, Cu, and Co ions through carboxylic groups.[29] Also Fe/histidine 1:1 complexes have been reported to have a metal equilibrium constant of 4.7.[30]

Conclusions

The pH range of Fe-loaded Nafion in the Orange II discoloration has been extended up to 10.2 through the development of an innovative catalyst of Fe/histidine prepared in situ on the Nafion. This avoids the expensive initial pH adjustment in Fenton homogeneous reactions. This finding is significant for the practical problem of dye discoloration. Since the Fe/histidine species is positively charged, it attaches electrostatically to the sulfonic groups of the Gierke cages in the Nafion. The immobilization step seems to increase the stability of this complex. The catalysts tested did not show any loss of activity during long-term use during Orange II degradation. The Fe/histidine/Nafion membrane was observed to be resistant to oxidative radical attack by the radicals generated in solutions up to 30 mm H_2O_2 at acid, neutral, and basic pH values (10.2).

Acknowledgment. This work was supported by the following: grant CTI/KTI TOP NANO-21 No. 6116.4 and grant No. OFES No. CO2.0068 COST D19 (Bern, Switzerland). We thank D. Laub and P. A. Buffat (CIME, EPFL) for their help with the TEM work.

References and Notes

(1) Fernandez, J.; Bandara, J.; Lopez, A.; Albers, P.; Kiwi, J. *Chem. Commun.* **1998**, 1493.
(2) Fernandez, J.; Bandara, J.; Lopez, A.; Albers, P.; Kiwi, J. *Langmuir* **1999**, *15*, 185.
(3) Benkelberg, H.; Warneck, P. *J. Phys. Chem.* **1995**, *99*, 5214.
(4) Sychev, A.; Isak, V. *Russ. Chem. Rev.*, **1995**, *64*, 1105.
(5) Faust, B.; Hoigne, J. *Atmos. Environ.* **1990**, *23*, 235.
(6) Ruppert, G.; Bauer, G.; Heisler, G. *J. Photochem. Photobiol, A, Chem.* **1993**, *73*, 75.
(7) Walling, C. *Acc. Chem. Res.* **1975**, *12*, 125.
(8) Halmann, M. *Photodegradation of Organic Pollutants*; CRC Press: Boca Raton, Florida, 1996.
(9) Nadtochenko, V.; Kiwi, J. *J. Chem. Soc., Faraday Trans.* **1997**, *93*, 2373.
(10) Kiwi, J.; Denisov, Y.; Gak, N.; Ovanesyan N.; Buffat, P.; Titov, A.; Sarkisov, O.; Albers, P.; Nadtochenko, V. *Langmuir*, **2002**, *23*, 9054.
(11) Gozzo, F. *J. Mol. Catal. A: Chem.* **2001**, *171*, 1.
(12) Isak, V.; van Suen, N.; Sychev, Y. *Russ. J. Phys. Chem.* **1980**, *54*, 282.
(13) Premkumar, J.; Ramaraj, R. *J. Mol. Catal. A: Chem.* **1998**, *32*, 21.
(14) Yagi, M.; Kasamastu, M.; Kaneko, M. *J. Mol. Catal. A: Chem.* **2000**, *151*, 29.
(15) Seen, A.; Townsend, A.; Bellis, J.; Cavell, K. *J. Mol. Catal. A: Chem.* **1999**, *149*, 233.
(16) Zhao, F.; Zhang, J.; Kaneko, M. *J. Photochem. Photobiol. A: Chem.* **1998**, *119*, 53.
(17) Stookey, L. *Anal. Chem.* **1970**, *42*, 779.
(18) Harrick, J. *Internal Reflection Spectroscopy*; Harrick Scientific: Ossinning, New York, 1987.

(19) DIN Norms 319, National Physics Laboratory, Teddington, UK, 1982.
(20) Shirley, A. *Phys. Rev.* B5, **1979**, 4709.
(21) (a) Kalyanasundaram, K. *Photochemistry of Polypyridine and Porphyrin Complexes*; Academic Press: London, UK, 1992. (b) Kalyanasundaram, K., Thomas, J. *J. Phys. Chem*. **1977**, *81*, 2176.
(22) Dhananjeyan, M.; Kiwi, J.; Albers, P.; Enea, O. *Helv. Chim. Acta*, **2001**, *85*, 3433.
(23) Safarzade-Amiri, A.; Bolton, J.; Cater, A. *J. Adv. Oxid. Technol*. **1995**, *1*, 18.
(24) Laporta, M.; Pegoraro, M.; Zanderighi, I. *Phys. Chem. Chem. Phys*. **1999**, *1*, 4619.
(25) Dragone, R.; Galli, P.; Massucci, M.; Tombetta, M. *J. Mater. Chem*. **2003**, *13*, 834.
(26) Harmer, M.; Farneth, W.; Sun, Q. *J. Am. Chem. Soc*. **1996**, *118*, 7708.
(27) Bozzi, A.; Yuranova, T.; Mielczarski, E.; Mielczarski, J.; Buffat, P.; Lais, P.; Kiwi, J. *Appl. Catal. B*. **2003**, *42*, 289.
(28) Bozzi, A.; Yuranova, T.; Mielczarski, J.; Lopez, A.; Kiwi, J. *Chem. Comm*. **2002**, 2202.
(29) Sundberg, R.; Martin R. *Chem. Rev.* **1974**, *74*, 471.
(30) Martell, E.; Smith, R. *Critical Stability Constants*; Plenum Press: London, 1984.
(31) Bandara, J.; Kiwi, J. *New J. Chem*. **1999**, *23*, 717.